C-type lectin signaling in dendritic cells: molecular control of antifungal inflammation

Wevers, B.A.

Publication date
2014

Partly cloudy on jupiter

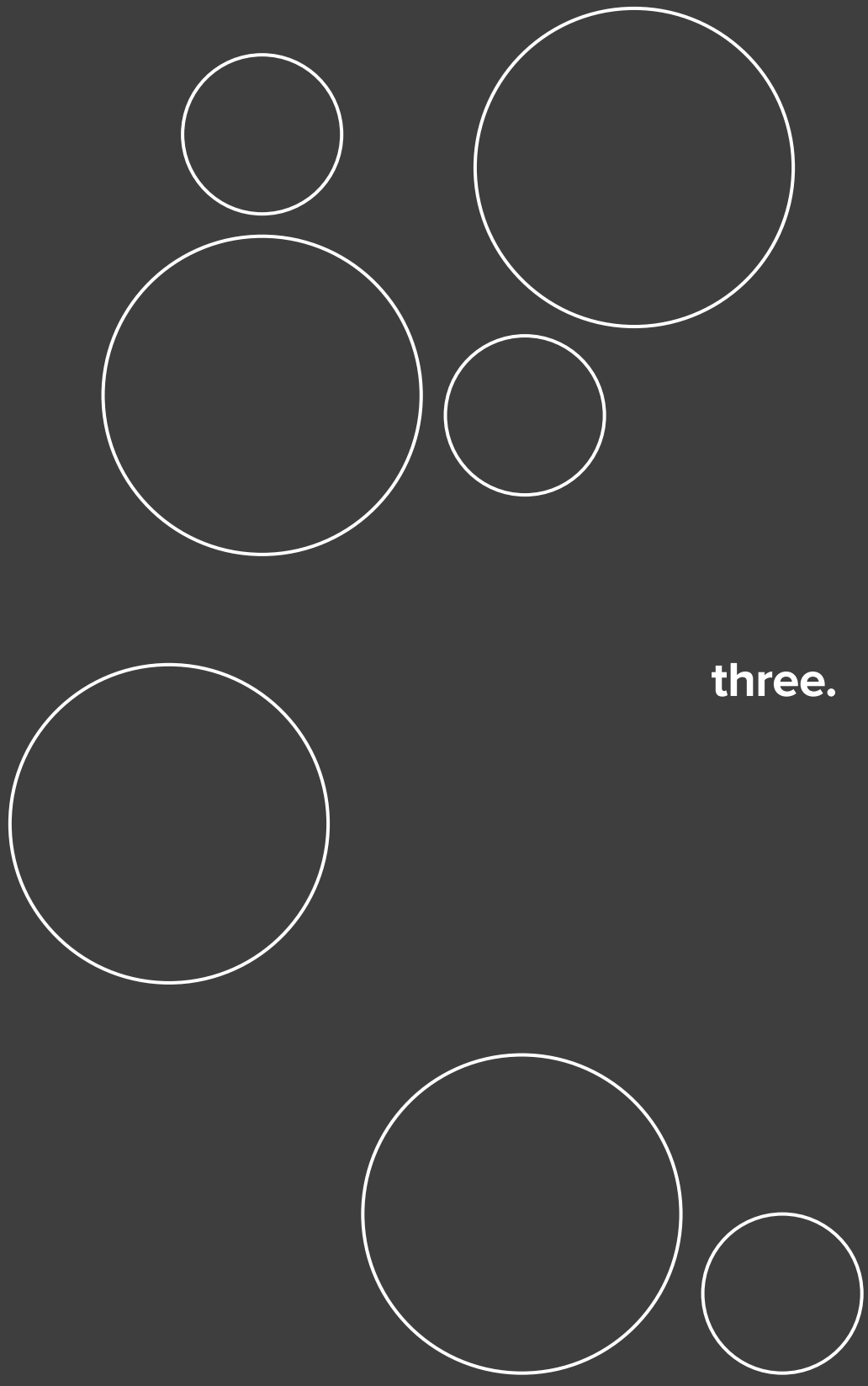
three.

three.

Fungal engagement of the C-type lectin mincle suppresses dectin-1-induced antifungal immunity

Cell Host Microbe, 15; 494-505 (2014)

Brigitte A. Wevers[1], Tanja M. Kaptein[1], Esther M. Zijlstra-Willems[1], Bart Theelen[2], Teun Boekhout[2], Teunis B.H. Geijtenbeek[1] and Sonja I. Gringhuis[1]

[1]Department of Experimental Immunology, Academic Medical Center, University of Amsterdam, Amsterdam, NL.
[2]Centraal bureau voor schimmelcultures, Utrecht, NL.

Recognition of fungal pathogens by C-type lectin receptor (CLR) dectin-1 on human dendritic cells is essential for triggering protective antifungal TH1 and TH17 immune responses. We show that *Fonsecaea monophora*, a causative agent of chromoblastomycosis, a chronic fungal skin infection, evades these antifungal responses by engaging CLR mincle and suppressing IL-12, which drives TH1 differentiation. Dectin-1 triggering by *F. monophora* activates transcription factor IRF1, which is crucial for *IL12A* transcription via nucleosome remodeling. However, simultaneous *F. monophora* binding to mincle induces an E3 ubiquitin ligase Mdm2-dependent degradation pathway, via Syk-CARD9-mediated PKB signaling, that leads to loss of nuclear IRF1 activity, hence blocking *IL12A* transcription. The absence

INTRODUCTION

Fungal species are ubiquitously present and pose considerable risk to human health. While opportunistic fungi cause disease in vulnerable patient groups, particular fungal strains are virulent regardless of host immunocompetence. Dendritic cells (DCs) have a key role in the generation of protective antifungal immunity by orchestrating activation and expansion of $CD4^+$ effector T cell populations that restrict fungal growth and enable phagocytic clearance[1]. Efficient host protection to fungi requires a coordinated immune response consisting of T helper cell (T_H) type 1 and T_H17 cells[2-4]. Both T_H1 and T_H17 cells are involved in chemotaxis and activation of phagocytes, particularly macrophages and neutrophils, via secretion of interferon-γ (IFN-γ) and IL-17, respectively[5,6]. T_H1-produced IFN-γ is essential for optimal activation of phagocytic effector cell functions, e.g. release of nitric oxide and production of reactive oxygen intermediates, to combat fungal persistence[7]. The critical role of T_H1 cells is underscored by the susceptibility of IFN-γ knockout mice to fungal infections[8] and the successful use of IFN-γ therapy in controlling human mycoses[9].

Chromoblastomycosis is a chronic progressive fungal infection of skin and subcutaneous tissue that occurs worldwide and is caused by traumatic inoculation of a specific group of dematiaceous fungi, most commonly *Fonsecaea*, *Cladophialophora* and *Phialophora* species[10]. Fungal strains that cause chromoblastomycosis are highly pathogenic and affect immunocompetent hosts[11]. Lesions of chromoblastomycosis

of IL-12 leads to impaired T_H1 responses and promotes T_H2 polarization. Notably, mincle is similarly exploited by other chromoblastomycosis-associated fungi to redirect T_H responses. Thus, mincle is a fungal receptor that can suppress antifungal immunity and, as such, is a potential therapeutic target.

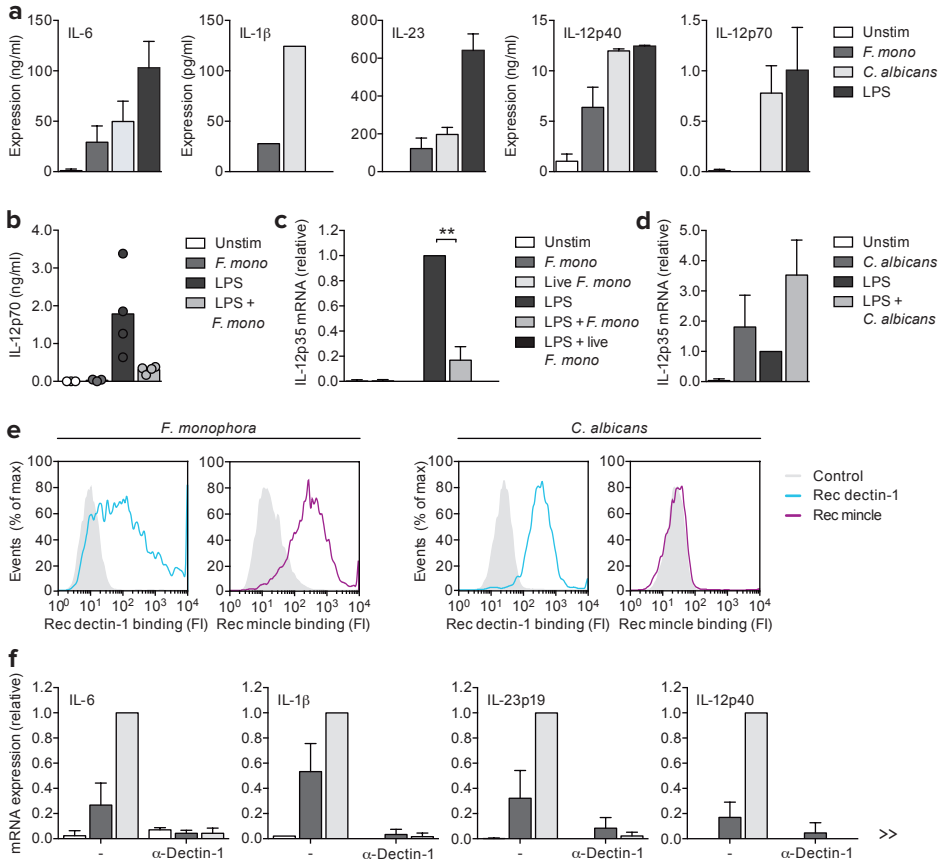

Figure 1. Fonsecaea monophora induces cytokine expression via dectin-1, while mincle signaling selectively suppresses IL-12p35 expression. (a,b,g) Cytokine secretion in supernatants of DCs 24 h after stimulation with curdlan, LPS and/or heat-killed *F. monophora* or *C. albicans* measured by ELISA. In (g), DCs are from a donor lacking functional dectin-1 due to a homozygous dectin-1 Y238X mutation. In (a,g), data are presented as mean ± SD of duplicate samples. (c,d,f,h,i) Cytokine mRNA expression by DCs 6 h after stimulation with LPS and/or heat-killed or live *F. monophora*, heat-killed *Candida albicans* or TDB, ⊙

patients that manifest a high fungal load are characterized by the presence of TH2 cells[12]. TH2 cells are detrimental for antifungal defense as they oppose fungal elimination[3], suggesting that these fungi have evolved to escape or manipulate innate and adaptive immune responses.

C-type lectin receptors (CLRs), a prominent class of pathogen recognition receptors (PRRs), expressed on DCs couple innate recognition of fungal carbohydrates to expression of cytokines involved in Th polarization[13]. Interleukin (IL)-12p70 is crucial for differentiation

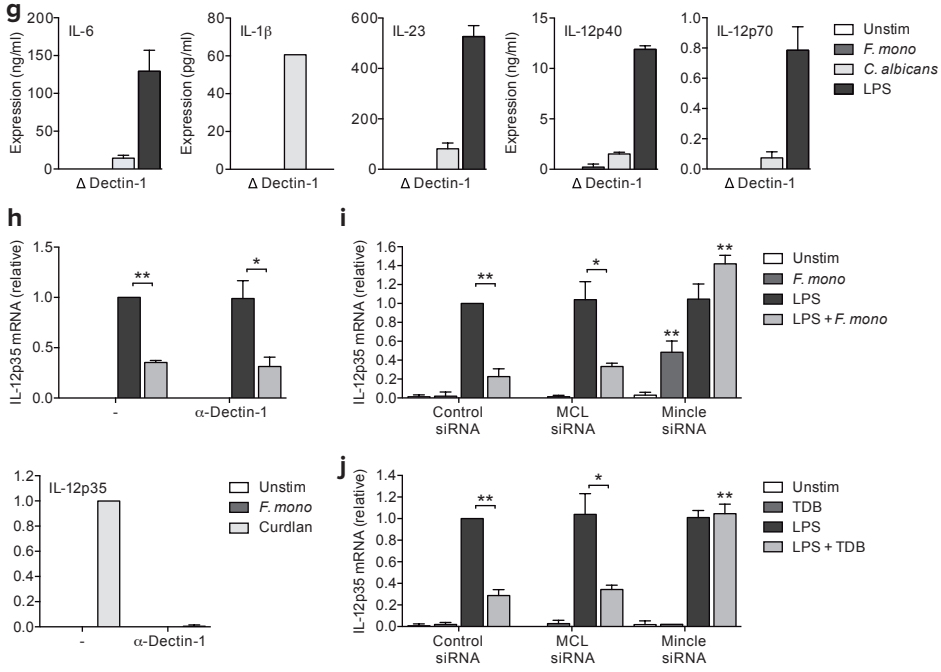

in the absence or presence of blocking dectin-1 antibodies (f) or after mincle or MCL silencing (h,i) by RNA interference (siRNA), measured by real-time PCR, normalized to GAPDH and set at 1 in LPS- (c,d,h,i) or curdlan (f)-stimulated cells. Data are presented as mean ± SD. *$P < 0.05$; **$P < 0.01$. (e) Binding of recombinant dectin-1 (*blue*) or mincle (*pink*) protein to heat-killed *F. monophora* or *C. albicans* conidia, determined by flow cytometry (FI, fluorescence intensity). Data are representative of at least two (a,e,g), three (d,f,h,i), four (b) or six (c) independent experiments.

of TH1 cells[14], while activation and maintenance of TH17 cells by DCs requires secretion of IL-1β together with IL-6 and IL-23[6,15]. CLR-induced signaling pathways that induce human antifungal Th polarization programs are now being defined. Dectin-1 is an important fungal sensor and dectin-1 triggering activates Syk, which induces assembly of a signaling complex consisting of CARD9, Bcl-10 and MALT1[16], resulting in activation of both classical and noncanonical NF-kB pathways to induce expression of TH1- and TH17-polarizing cytokines[17]. Recently, CLR mincle has been reported to be involved in host responses against several

fungi, including *Malassezia*, some *Candida* species and *Fonsecaea pedrosoi*[11,18,19], however its contribution to antifungal immunity remains unclear. Mincle transduces Syk-CARD9 signaling via the paired Fc receptor common γ-chain (FcRγ) adaptor[20-22]. Mincle can heterodimerize with another C-type lectin, macrophage C-type lectin (MCL), forming a functional trimeric receptor complex with FcRγ[23]. In mice, mincle agonists promote induction of TH1 and TH17 responses[24]. However, how human mincle affects cytokine transcription and subsequently TH differentiation remains unclear.

Here we identify mincle as a suppressor of DC-driven antifungal defenses by suppression of IL-12 production. We show that interferon regulatory factor 1 (IRF1) is crucial for IL-12 production by inducing nucleosome remodeling of *IL12A*. Dectin-1 triggering by *F. monophora* induced IRF1-dependent IL-12p35 mRNA expression but, notably, our study demonstrates that *F. monophora* simultaneously triggered mincle, which led to specific degradation of IRF1, thereby suppressing *IL12A* transcription. Mincle induced a signaling cascade that led to E3 ubiquitin ligase Mdm2-dependent proteasomal degradation of IRF1 in the nucleus. Suppression of IL-12p70 biosynthesis redirected TH differentiation from TH1 to TH2 responses, thereby adversely affecting antifungal defense mechanisms. Thus, human mincle is a prominent modulator of antifungal immunity and immune suppressor, and might be targeted to treat chromoblastomycosis as well as disorders characterized by aberrant IL-12-driven inflammation, such as autoimmune diabetes.

RESULTS

***F. monophora* selectively represses IL-12p35 production in human DCs.** Stimulation of primary human DCs with heat-killed conidia from chromoblastomycosis isolate *F. monophora* induced expression of maturation markers CD80, CD86, CD83 and MHC class II DR (HLA-DR) (Figure S1). Furthermore, *F. monophora* induced expression of IL-6, IL-1β, IL-23 and IL-12p40, but not IL-12p70 by DCs (Figure 1a). Next, we examined the lack of IL-12p70 expression. Whereas TLR4 triggering by lipopolysaccharide (LPS) induced strong IL-12p70 secretion, simultaneous stimulation with *F. monophora* severely suppressed LPS-mediated IL-12p70 release (Figure 1b). IL-12p70 is a heterodimeric cytokine, comprising of IL-12p35 and IL-12p40 subunits[25]. *F. monophora*-stimulated DCs produced IL-12p40 as well as bioactive IL-23, which consists of IL-12p40 and IL-23p19 subunits (Figure 1a), indicating that IL-12p70 expression is restricted at the level of IL-12p35 mRNA. *F. monophora* alone failed to trigger IL-12p35 expression, while LPS-induced IL-12p35 mRNA levels were significantly blocked after coexposure to *F. monophora* (Figure 1c). The *F. monophora*-mediated suppression of LPS-induced IL-12p35 mRNA expression was even more evident when live fungi were used (Figure 1c). In contrast, *Candida albicans* strongly induced IL-12p35 responses, and enhanced LPS-induced IL-12p35 mRNA expression (Figure 1d). These data strongly

suggest that *F. monophora* actively suppresses IL-12p35 production.

***F. monophora* targets mincle to inhibit IL-12p35 expression.** We next set out to identify the innate receptor(s) involved in *F. monophora* responses and IL-12p35 suppression. Dectin-1 is an important receptor for fungi such as *C. albicans* and recombinant human dectin-1 interacted with *F. monophora* to a comparable level as *C. albicans* (Figure 1e). We next investigated whether dectin-1 is involved in cytokine responses to *F. monophora*. Blocking antibodies against dectin-1 abrogated *F. monophora*-induced IL-6, IL-1β, IL-23p19, and IL-12p40 mRNA expression, as were the responses induced by dectin-1 agonist curdlan (Figure 1f). Moreover, DCs derived from a donor carrying a homozygous Y238X dectin-1 mutation, hence lacking functional dectin-1 expression [26] (Figure S2), did not produce IL-6, IL-1β, IL-23 and IL-12p70 after stimulation with *F. monophora* (Figure 1g and S2). In contrast, both LPS and *C. albicans* (strain CBS2712, which is not strictly dependent on dectin-1 for triggering cytokine responses[27]) induced cytokines in the absence of functional dectin-1 (Figure 1g). Furthermore, blocking dectin-1 signaling did not interfere with *F. monophora*-mediated suppression of LPS-induced IL-12p35 mRNA expression (Figure 1h). These data strongly suggest that dectin-1 recognition of *F. monophora* is crucial for induction of cytokine gene transcription, whereas another innate receptor is responsible for the suppression of IL-12p35.

We found that *F. monophora*, in contrast to *C. albicans*, interacted with recombinant human mincle (Figure 1e). As mincle is constitutively expressed on human immature DCs (Figure S2), we investigated whether mincle is involved in IL-12p35 suppression by *F. monophora*, by silencing mincle expression in DCs by RNA interference (Figure S3). Strikingly, mincle silencing restored IL-12p35 mRNA and IL-12p70 protein expression in response to *F. monophora*, without affecting curdlan-induced IL-12p35 synthesis (Figure 1i and S4). Furthermore, mincle silencing restored LPS-induced IL-12p35 mRNA and IL-12p70 protein expression in the presence of *F. monophora* (Figure 1i and S4). We determined next whether the suppressive effect of mincle on IL-12p35 expression required the presence of MCL, as mincle can heterodimerize with MCL to form functional complexes with FcRγ[23]. Silencing of MCL did not interfere with mincle surface expression, while, vice versa, mincle silencing only slightly affected cell surface expression of MCL (Figure S3). Importantly, silencing of MCL did not interfere with IL-12p35 suppression by *F. monophora* (Figure 1i), indicating that the suppression is independent of MCL.

To further examine the involvement of mincle in IL-12p35 suppression, we used trehalose-6,6-dibehenate (TDB), a known mincle and MCL agonist[20,28]. Similar to *F. monophora* stimulation, triggering of DCs by TDB alone failed to induce IL-12p35 mRNA, but suppressed LPS-induced IL-12p35 mRNA expression (Figure 1j). Mincle silencing effectively prevented repression of LPS-induced IL-12p35 mRNA expression by TDB, whereas MCL silencing did not interfere with the suppressive effect of TDB (Figure 1j). Taken together, these data demonstrate that dectin-1 induces cytokines in response to *F. monophora*, whereas mincle

signaling suppresses transcription of IL-12p35.

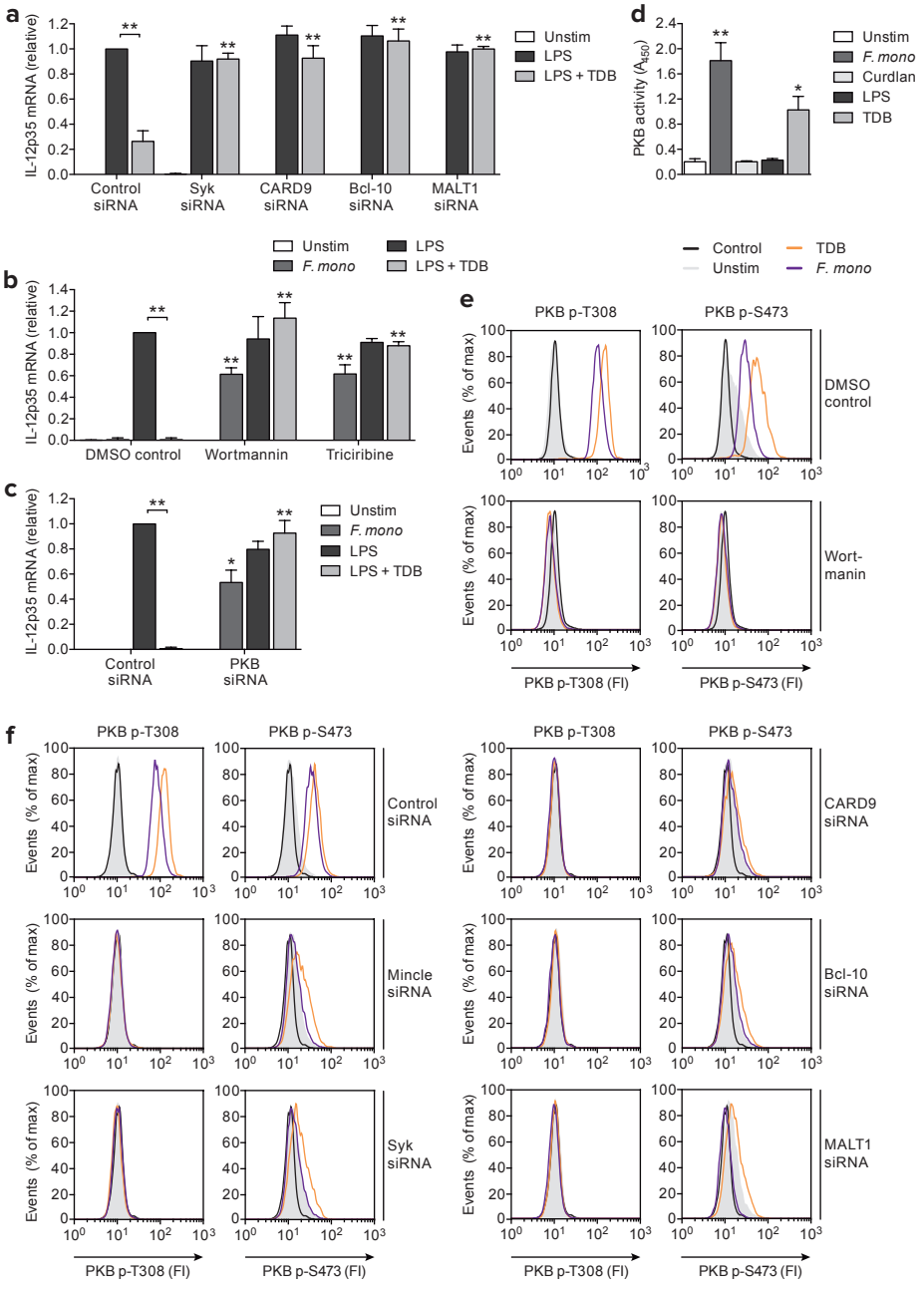

Mincle signaling suppresses IL-12p35 expression via PKB activation. We set out to elucidate the mechanism behind mincle-mediated IL-12p35 suppression. As both dectin-1 and mincle signal via Syk-CARD9[16,22], we combined TLR4 triggering with selective mincle stimulation by TDB to distinguish between dectin-1- and mincle-mediated effects. Silencing of Syk, CARD9, Bcl-10 or MALT1 abrogated the suppressive effects of TDB on LPS-induced IL-12p35 expression (Figure 2a), demonstrating that mincle suppresses IL-12p35 via Syk-CARD9-Bcl-10-MALT1-mediated signaling. To further identify mincle-specific downstream targets, we utilized a panel of small molecule inhibitors. We noted in particular that pretreatment of DCs with wortmannin, an irreversible inhibitor of PI3K, abrogated IL-12p35 suppression by TDB and restored expression to LPS-induced levels (Figure 2b). Similarly, inhibition of PKB (or Akt), a well-established effector of PI3K, by small molecule inhibitor triciribine (Figure 2b) or PKB silencing (Figure 2c), blocked TDB-mediated suppression of IL-12p35. Thus, the PI3K-PKB cascade plays a primary role in mincle-mediated IL-12p35 suppression. Indeed, TDB, in contrast to curdlan or LPS, strongly induced PKB kinase activity (Figure 2d). PKB activation requires phosphorylation at Thr308 and Ser473, which is controlled by PI3K via kinases PDK1 and mTORC2, respectively[29]. Mincle stimulation led to PKB phosphorylation at both Thr308 and Ser473 (Figure 2e), while LPS and curdlan had no effect (Figure S5), correlating with PKB activity (Figure 2d). PKB phosphorylation after TDB stimulation was dependent on PI3K activity (Figure 2e) as well as mincle and mincle-mediated signaling via the Syk-CARD9-Bcl-10-MALT1 module as silencing of these proteins inhibited TDB-induced PKB phosphorylation (Figure 2f). Furthermore, we found that *F. monophora* induced PI3K-dependent PKB phosphorylation via mincle (Figure 2e and 2f), which relied on Syk and the CARD9-Bcl-10-MALT1 scaffold (Figure 2f). These results indicate that mincle suppresses dectin-1-induced IL-12p35 expression in response to *F. monophora* by activation of PI3K-PKB signaling, through a Syk-CARD9-Bcl-10-MALT1-dependent pathway.

Figure 2. Mincle signaling suppresses IL-12p35 expression via PI3K and PKB. (a-c) IL-12p35 mRNA expression by DCs 6 h after stimulation with LPS and/or TDB or *F. monophora* after Syk, CARD9, Bcl-10, MALT1 or PKB silencing (a,c), or in the absence or presence of PI3K inhibitor wortmannin or PKB inhibitor triciribine (b), measured by real-time PCR, normalized to GAPDH and set at 1 in LPS-stimulated cells. Data are presented as mean ± SD. $*P < 0.05$; $**P < 0.01$. (d) PKB kinase activity in whole cell lysates of DCs after 30 min of stimulation with curdlan, *F. monophora*, LPS and/or TDB. Data are presented as mean ± SD. $*P < 0.05$; $**P < 0.01$. (e,f) PKB phosphorylation at Thr308 or Ser473 in DCs left unstimulated (*grey*) or 20 min after stimulation with TDB (*orange*) or *F. monophora* (*purple*), in the absence or presence of PI3K inhibitor wortmannin (e), or after mincle, Syk, CARD9, Bcl-10 or MALT1 silencing (f), determined by flow cytometry (FI, fluorescence intensity). Data are representative of at least three (a-f) independent experiments.

Mincle signaling impairs nucleosome remodeling at the IL12A promoter. *IL12A* transcription is rigidly controlled; in resting cells, the *IL12A* promoter is assembled into stable nucleosomes, whereas upon stimulation, repositioning of nucleosome 2 (nuc-2) allows binding of, among others, transcription factor NF-kB and subsequent transcriptional initiation by RNA polymerase II (RNAPII)[30]. We observed that, although *F. monophora* interfered with recruitment of NF-kB p65 to the *IL12A* promoter (Figure 3a), fungal stimulation did not abrogate nuclear translocation and DNA binding of p65 (Figure 3b). Indeed, *F. monophora* alone induced nuclear translocation of p65, c-Rel and RelB (Figure 3b), which are a hallmark of dectin-1 signaling[17]. RNAPII recruitment to the *IL12A* promoter was almost completely abolished as determined by chromatin immunoprecipitation (ChIP) assays (Figure 3a). Since these data suggest that mincle signaling interferes with *IL12A* transcription prior to RNAPII and NF-kB binding, we next examined whether *F. monophora* interferes with *IL12A* nucleosome remodeling, using a chromatin accessibility real-time PCR (ChART) assay specific for nuc-2 repositioning[31]. *F. monophora* did not induce *IL12A* nucleosome remodeling, whereas curdlan and LPS evoked complete remodeling (Figure 3c). Notably, LPS-induced *IL12A* nucleosome remodeling was severely diminished when DCs were costimulated with *F. monophora* (Figure 3c), while silencing of mincle restored LPS-induced *IL12A* nucleosome remodeling (Figure 3d). These results strongly suggest that *F. monophora*–induced mincle signaling inhibits IL-12p35 expression by interfering with nucleosome remodeling events indispensable for transcriptional activation at the *IL12A* promoter.

Mincle-induced PKB signaling blocks nuclear IRF1 activity. IRF1 is thought to be involved in transcriptional regulation of IL-12p35 expression; the nuc-2 promoter region of *IL12A* contains a centrally positioned IFN-stimulated response element (ISRE) that can be bound by IRF1[32]. IRF1 silencing abrogated IL-12p35 expression in response to curdlan or LPS stimulation (Figure 4a). In accordance, both dectin-1 and TLR4 triggering induced IRF1 recruitment to the ISRE site within the proximal *IL12A* promoter (Figure 4b). Strikingly, IRF1 silencing completely abrogated *IL12A* nucleosome remodeling induced by dectin-1 and TLR4 signaling (Figure 4c), which coincided with impaired recruitment of RNAPII and p65 to the *IL12A* promoter (Figure 4d). These data show that IRF1 plays an essential role in *IL12A* transcription in response to both dectin-1 and TLR4 via nucleosome remodeling.

We next investigated whether mincle triggering affects *IL12A* nucleosome remodeling by interfering with IRF1 activation. We found that both curdlan and LPS induced nuclear translocation of IRF1 (Figure 4e). Remarkably, simultaneous stimulation with *F. monophora* completely abrogated LPS-induced nuclear IRF1 accumulation (Figure 4f). *F. monophora* alone did not induce nuclear IRF1 accumulation (Figure 4f). Also, we observed a complete absence of nuclear IRF1 after TLR4 and mincle costimulation (Figure 4g and 4h). Silencing of either mincle or downstream effector PKB restored nuclear IRF1 accumulation after LPS and TDB costimulation as well as *F. monophora* stimulation, without affecting LPS-induced

nuclear IRF1 accumulation or cytoplasmic IRF1 expression (Figure 4i). These data show that PKB-mediated mincle signaling restricts nuclear accumulation of IRF1, suggesting that this mechanism underlies the block in *IL12A* nucleosomal remodeling and subsequent transcription in response to *F. monophora*.

Mincle directs proteasomal degradation of nuclear IRF1 via Mdm2. Since IRF1 steady-state levels are tightly controlled by a balance between synthesis and ubiquitin-mediated proteolysis[33,34], we investigated whether mincle interferes with IRF1 by inducing its degradation. Treatment with proteasome inhibitor MG-132 reversed the block in nuclear IRF1 accumulation in response to LPS and TDB costimulation (Figure 5a), indicating that IRF1 is indeed

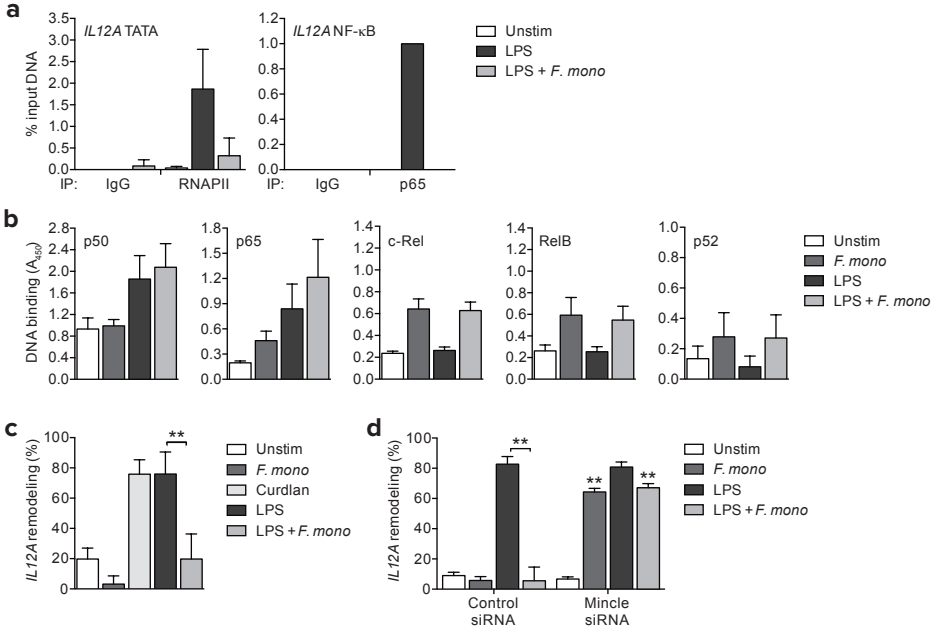

Figure 3. Mincle signaling blocks *IL12A* transcription via PKB by inhibition of nucleosome remodeling. (a) RNA polymerase II (RNAPII) and p65 recruitment to TATA box and NF-κB binding motifs of the *IL12A* promoter in DCs 2 h after stimulation with LPS and/or *F. monophora*, determined by ChIP assay. IgG indicates a negative control. Data are expressed as % input DNA and presented as mean ± SD. (b) NF-κB subunit activation in nuclear extracts of DCs 2 h after stimulation with LPS and/or *F. monophora*, measured by DNA binding ELISA. Data are presented as mean ± SD. (c,d) *IL12A* nucleosome remodeling in DCs 3 h after stimulation with curdlan, LPS and/or *F. monophora* or TDB, after mincle silencing (d), determined by ChART assay and normalized to GAPDH. Data are expressed as % remodeling and presented as mean ± SD. $^{**}P < 0.01$. Data are representative of at least four (a; p65), three (a; RNAPII, B-D) independent experiments.

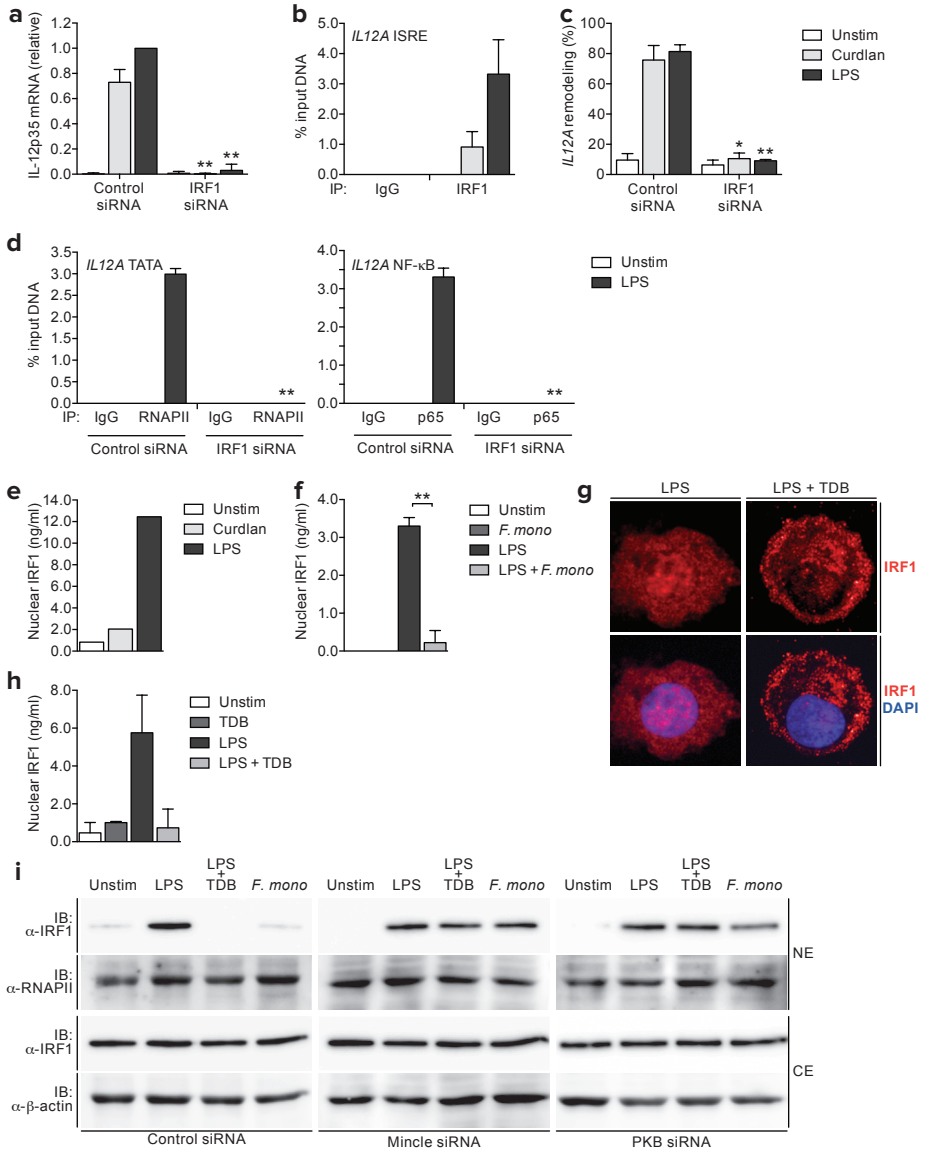

Figure 4. Mincle signaling suppresses nuclear IRF1 to block *IL12A* nucleosome remodeling. (a) IL-12p35 mRNA expression by DCs 6 h after stimulation with curdlan or LPS, after IRF1 silencing, measured by real-time PCR, normalized to GAPDH and set at 1 in LPS-stimulated cells. Data are presented as mean ± SD. $^{**}P < 0.01$. (b,d) IRF1 (b), RNAPII and p65 (d) recruitment to ISRE binding site (b), TATA box or NF-κB binding motif (d) of the *IL12A* promoter in DCs 2 h after stimulation with curdlan or LPS (b,d), after IRF1 silencing (d), determined by ChIP assay. IgG indicates a negative control. Data are expressed as % input DNA and presented as mean ± SD. $^{**}P < 0.01$. (c) *IL12A* nucleosome remodeling in DCs 3 h after stimulation with curdlan or LPS, after IRF1 silencing, determined by ChART assay and normalized to GAPDH. Data are ⊙

targeted for proteasomal degradation by mincle. Since PKB has been shown to induce the E3 ubiquitin ligase activity of Mdm2, which has recently been reported to aid in IRF1 proteasomal degradation[33,35,36], we explored a possible Mdm2 contribution. Remarkably, Mdm2 silencing completely abrogated mincle-mediated IL-12p35 suppression in response to TDB and *F. monophora*, without affecting LPS-induced IL-12p35 expression (Figure 5b). To regulate IRF1, Mdm2 must gain nuclear entry, a process which requires phosphorylation of Mdm2 at Ser166 by PKB[35,36]. We found that mincle triggering by both TDB and *F. monophora*, but not TLR4 triggering, induced nuclear translocation of Mdm2 (Figure 5c). Only Mdm2 present within the nucleus was phosphorylated at key residue Ser166 (Figure 5c). Mdm2 Ser166 phosphorylation following TDB and *F. monophora* stimulation was abrogated by silencing of mincle, Syk, CARD9, Bcl-10 and MALT1, or chemical inhibition of PI3K or PKB (Figure 5d and S5). Similarly, mincle and PKB silencing blocked Mdm2 nuclear translocation (Figure 5c). TDB-induced Mdm2 phosphorylation and nuclear translocation was not affected by LPS stimulation (Figure 5c and S5). Since the E3 ubiquitin ligase activity of Mdm2 relies on association with its substrates[37,38], we prepared nuclear extracts in the presence of MG-132 to block degradation, allowing us to determine whether Mdm2 interacts with IRF1 within the nucleus. We found that nuclear IRF1 immunoprecipitated together with Mdm2 in both TDB- and *F. monophora*-, but not LPS-stimulated DCs (Figure 5e). The importance of Mdm2 in IRF1 regulation was further supported by data showing that silencing of Mdm2 prevented IRF1 degradation after mincle triggering (Figure 5f). Taken together, these results demonstrate that mincle signaling induces Mdm2 activation and nuclear translocation in a PKB-dependent manner to target IRF1 for proteasomal degradation, accounting for the IL-12p35 antagonism observed after *F. monophora* stimulation.

Mincle signaling suppresses antifungal TH1 responses. IL-12 is crucial in TH1 cell differentiation. We next investigated how mincle-induced PKB-Mdm2-mediated IRF1 degradation affects antifungal Th differentiation. LPS-primed DCs directed Th polarization toward TH1 responses, whereas IRF1 silencing led to severely diminished TH1 responses after LPS stimulation (Figure 6a and 6b). Neutralizing antibodies against IL-12 impaired TH1 cell differentiation by LPS-primed DCs (Figure 6c and 6d), underlining the crucial role for IL-12 in

expressed as % remodeling and presented as mean ± SD. *$P < 0.05$; **$P < 0.01$. (e-i) IRF1 nuclear translocation in DCs 2 h after stimulation with curdlan, LPS and/or TDB or *F. monophora*, after mincle or PKB silencing (i), determined by ELISA on nuclear extracts (e,f,h), immunofluoresence microscopy (g; IRF1, red; DAPI, *blue*) or immunoblotting (i; nuclear, NE; cytoplasmic, CE extracts). In (i), RNAPII and β-actin served as loading controls for NE and CE, respectively. Data in (e,f,h) are presented as mean ± SD. *$P < 0.05$. Data are representative of at least three (a,c,d,f,h), two (b,g,i), one (e; curdlan) or five (e; LPS) independent experiments.

TH1 polarization. *F. monophora*-primed DCs failed to induce TH1 responses, but promoted potent TH2 polarization (Figure 6e and 6f), which is consistent with IL-12p70 suppression by *F. monophora*. Moreover, *F. monophora* strongly impaired LPS-induced TH1 cell differentiation, actively skewing polarization towards a response dominated by TH2 cells (Figure 6e and 6f). Notably, mincle silencing completely restored TH1 cell polarization by LPS plus *F. monophora*-primed DCs (Figure 6g). Thus, suppression of IL-12p70 secretion after mincle triggering by *F. monophora* is fundamental in redirecting antifungal TH1 responses to TH2 immunity.

Various other fungi, highly related to *F. monophora*, are also causative agents of chromoblastomycosis in humans[10]. We next investigated whether these fungi also target mincle to suppress antifungal immune responses. All tested strains were recognized by recombinant mincle protein (Figure 7a). Strikingly, the pathogenic strains, i.e. *F. pedrosoi*, *F. compacta* and *Cladophialophora carrionii*, strongly suppressed LPS-induced TH1 differentiation and skewed Th polarization towards a TH2 response (Figure 7b). We also observed that the virulent strains repressed IL-12p35 responses similar to *F. monophora* (Figure 7c), accounting for the observed TH redirection. Mincle silencing reversed skewing of TH2 differentiation of LPS-primed DCs toward TH1 polarization for all strains tested (Figure 7d). Collectively, these data demonstrate that virulent fungal pathogens involved in chromoblastomycosis exploit mincle on human DCs to attenuate TH1 responses and induced TH2 immunity via suppression of *IL12A* transcription, which might allow these fungi to establish chronic infection.

DISCUSSION

An essential aspect of host resistance to fungal infection is the requirement for TH1 and TH17 responses[3,4]. Here we have identified mincle as a suppressor of proinflammatory cytokine IL-12, which redirects immunity to fungal pathogens causing chromoblastomycosis from antifungal TH1 responses towards TH2 differentiation. At the molecular level, we identified IRF1 as the crucial factor for nucleosome remodeling at the proximal *IL12A* promoter that was induced by dectin-1. *F. monophora* fungi binding to mincle led to activation of a PI3K-PKB signaling cascade that directed Mdm2-mediated proteasomal degradation of IRF1. Loss of IRF1 interfered with *IL12A* nucleosome remodeling, thereby suppressing IL-12p70. Thus, mincle antagonizes dectin-1 signaling in response to chromoblastomycosis-related fungi to suppress protective TH1 immunity, which might contribute in establishing chronic subcutaneous infection.

This study adds to an emerging paradigm in which CLRs and other PRRs on DCs act together to bridge fungal microbe recognition and transduce collaborative signaling that determines the overall response deployed against fungal microbes[27,39]. In recent years,

dectin-1 has been revealed as the primary PRR in antifungal immunity, capable of orchestrating TH1 and TH17 immune responses independently of other PRRs[17,40]. Here we found that chromoblastomycosis isolate *F. monophora* also triggered dectin-1 signaling, which was a prerequisite for classical and noncanonical NF-κB activation and consequently expression of TH1- and TH17-polarizing cytokines. However, *F. monophora* induced a second pathway through mincle that interfered with dectin-1-induced IL-12p70 expression. The combined activation of dectin-1 and mincle by *F. monophora* led to a cytokine gene expression profile that prevented generation of protective TH1 immune responses, instead inducing adverse TH2 responses. Thus, the overall immune response to *F. monophora* is determined by cooperation between dectin-1 and mincle, with dectin-1 acting as the general instigator and mincle as the crucial determinant or director.

Deficiency of TH1 effector responses due to mincle-mediated suppression of IL-12p35 expression in human DCs was not restricted to infection with *F. monophora*, but extended to chromoblastomycosis isolates, *F. pedrosoi*, *C. carrionii* and *F. compacta*, suggesting a common mode of immune evasion in the human host. Mincle was previously shown to be involved in innate recognition of *F. pedrosoi* in mice, yet was incapable of controlling protective immunity[11]; in this mouse model of chromoblastomycosis, TLR engagement was found to be sufficient to revert the immune dysfunction. In contrast, in our human model, we observed that mincle suppressed TLR4-induced IL-12p70 expression. This discrepancy might reflect differences in host defense between mice and humans. Indeed, we observed several differences between expression and function of human and murine mincle. While mincle has been described as an inducible receptor on mouse bone marrow-derived DCs -via triggering of MCL[28], we detected constitutive expression of mincle on human immature DCs. Furthermore, while mincle and MCL form functional trimeric receptor complexes with FcRγ in rat primary cells[23], we found that the presence of MCL was neither required for mincle expression, surface localization nor mincle-mediated signaling induced by either *F. monophora* or TDB to suppress *IL12A* transcription. These studies suggest that mincle has evolved different functions in defense against fungi and further studies are required to understand the differences between its functions in mice and humans.

Mincle has previously been identified as a positive regulator of TH17 immunity with its role in the therapeutic TH17 adjuvancy of mycobacterial glycolipid TDM and its synthetic derivate TDB[24]. In these murine models, in addition to TH17 immunity, mincle-mediated adjuvancy translates into robust TH1 responses[24,41] Even though a TDB-containing *M. tuberculosis* subunit vaccine[42] entered clinical trial, the immune stimulatory actions of TDB and TDM have never been tested extensively in the human setting[43]. Our finding that mincle suppresses human TH1 immunity implies that utilizing mincle agonists as vaccine adjuvants should be considered with caution.

Another important finding of our study is the crucial and nonredundant role of IRF1 in *IL12A* nucleosome remodeling and regulation of IL-12p35 synthesis by different PRRs. We

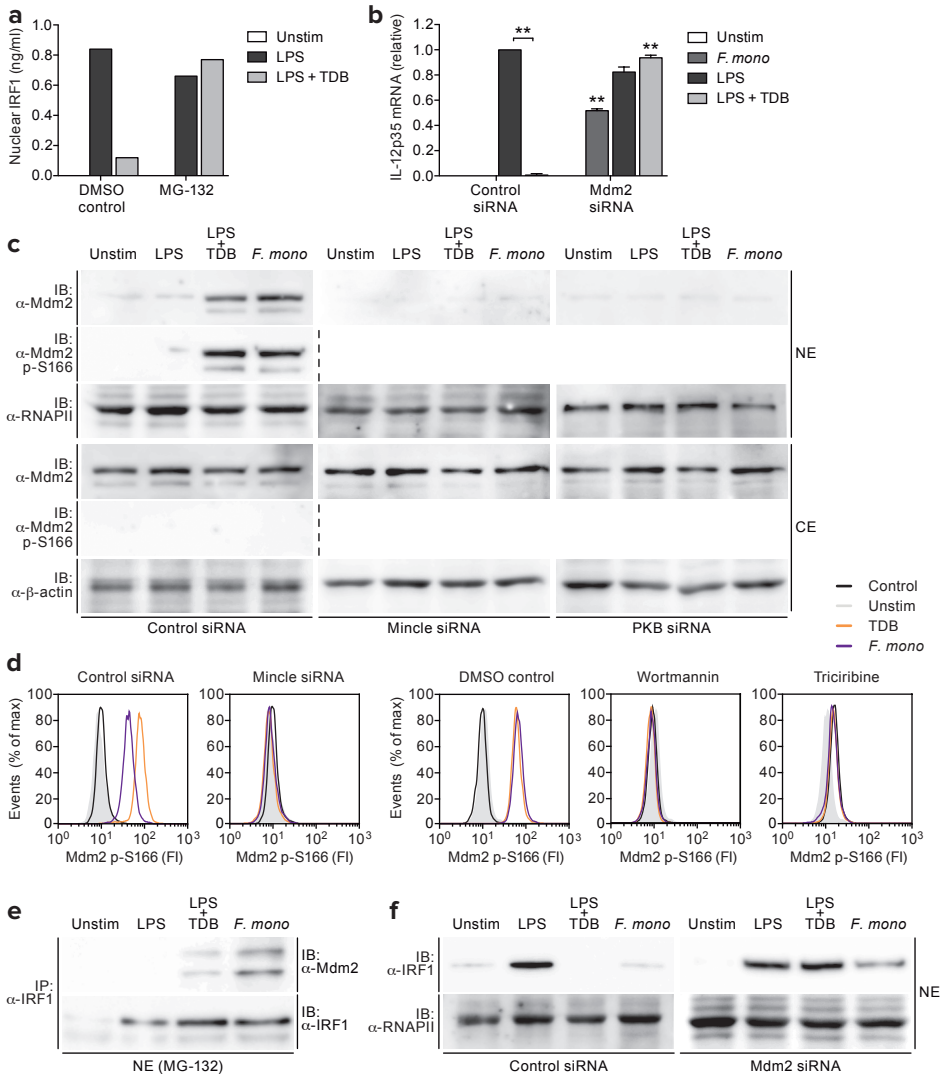

demonstrate that IRF1 is crucial for nucleosome remodeling of the proximal *IL12A* gene promoter in response to dectin-1 triggering, but also TLR4 ligation. IRF1-mediated *IL12A* nucleosome remodeling allows NF-kB subunit p65 and RNAPII recruitment, and hence productive *IL12A* transcription. Despite tight regulation of IRF1 transcriptional activity, with IRF1 steady-state levels constitutively restricted by ubiquitin-mediated proteolysis[33,34] and excess activation linked to cellular oncogenicity[44], the molecular aspects of IRF1 activation are yet to be delineated. TLR4-mediated IRF1 activation has been reported to be dependent on adaptor protein MyD88[45], yet how dectin-1 triggering leads to IRF1 activation remains to be resolved.

Figure 5. Mincle-PKB signaling induces proteasomal degradation of nuclear IRF1 via Mdm2. (a) IRF1 expression in nuclear extracts of DCs 2 h after stimulation with LPS and/or TDB or *F. monophora*, in the absence or presence of proteasome inhibitor MG-132, measured by ELISA. (b) IL-12p35 mRNA expression by DCs 6 h after stimulation with LPS and/or TDB or *F. monophora*, after Mdm2 silencing, measured by real-time PCR, normalized to GAPDH and set at 1 in LPS-stimulated cells. Data are presented as mean ±SD. $^{**}P < 0.01$. (c,f) Mdm2 (c) and IRF1 (f) cellular localization and Mdm2 phosphorylation at Ser166 (c) in DCs 2 h after stimulation with LPS and/or TDB or *F. monophora*, after mincle, PKB (c) or Mdm2 silencing (f), determined by immunoblotting (nuclear, NE; cytoplasmic, CE extracts). RNAPII and β-actin served as loading controls for NE and CE, respectively. (d) Mdm2 phosphorylation at Ser166 in DCs left unstimulated (*grey*) or 20 min after stimulation with TDB (*orange*) or *F. monophora* (*purple*), after mincle silencing, or in the absence or presence of PI3K inhibitor wortmannin or PKB inhibitor triciribine, determined by flow cytometry (FI, fluorescence intensity). (e) Mdm2 immunoprecipitated together with IRF1 (IP) from nuclear extracts of DCs 2 h after stimulation with LPS and/or TDB, or *F. monophora*, determined by immunoblotting (IB). NE were prepared in the presence of proteasome inhibitor MG-132 to block protein degradation. RNAPII served as loading control. Data are representative of at least two (a,c,e,f), or three (b,d) independent experiments.

Innate signaling by mincle interfered with nuclear IRF1 activity and abrogated IRF1-mediated *IL12A* remodeling. Our findings reveal that mincle exerted its suppressive effect by directing proteolytic breakdown of activated and nuclear localized IRF1, via Syk-CARD9-Bcl-10-MALT1-dependent activation of a PI3K-PKB cascade. We identified E3 ubiquitin ligase Mdm2 as the downstream effector: mincle-induced PKB activation led directly to Mdm2 phosphorylation and nuclear translocation. Mdm2 has previously been identified as a major negative regulator of numerous proteins involved in transcriptional regulation, most notably p53 and FOXO tumor suppressors, under conditions of physiological stress[37,38]. The association of Mdm2 with IRF1 within the nucleus targeted IRF1 for proteasomal degradation.

Activation of Syk to induce the assembly of the CARD9-Bcl-10-MALT1 or related CARD11-Bcl-10-MALT1 module is a common occurrence after receptor ligation. However, whereas dectin-1 and dectin-2 triggering induces NF-κB activation via this protein scaffold[16,17], mincle triggering uniquely coupled CARD9-Bcl-10-MALT1-mediated signaling to the PI3K-PKB cascade, without triggering NF-κB activation (unpublished data). The mechanisms underlying the fundamental differences between dectin-1, dectin-2 and mincle signaling despite the use of common signaling modules remain elusive. PKB has also been shown to be involved in antigen receptor signaling, where it modulates CARD11-Bcl-10-MALT1-induced NF-κB activation[46]. Our data now show the existence of a bidirectional relation between CARD9/CARD11-Bcl-10-MALT1 and PKB signaling that regulates immune responses.

Our results define IRF1 as a crucial player in antifungal T_H1 responses induced by human DCs via its role in IL-12p70 biosynthesis. Intriguingly, we found that mincle functions as a direct inhibitor of IRF1 nuclear activity and as such is commonly targeted by fungi causing

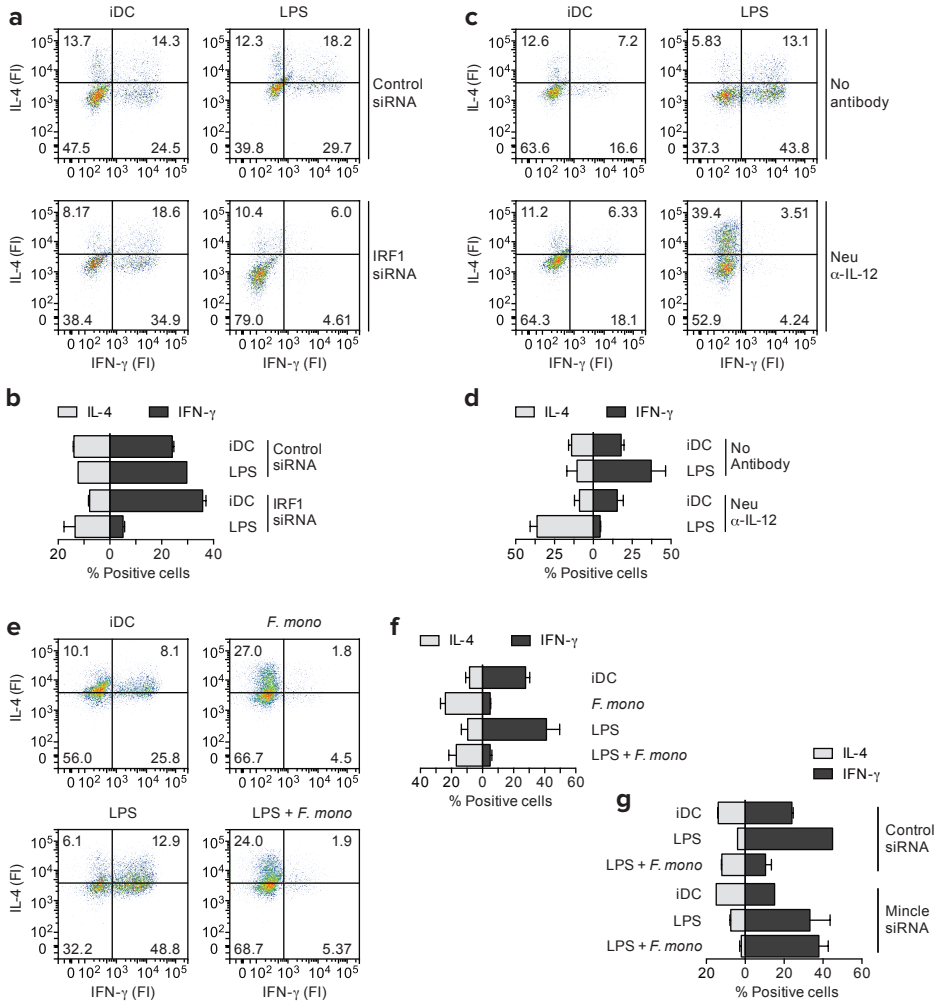

Figure 6. *F. monophora* targets mincle-induced IRF1 degradation to redirect antifungal TH1 polarization to TH2 responses. (a-g) T helper cell polarization was determined by flow cytometry by staining for intracellular IL-4 (TH2) or IFN-γ (TH1) expression after coculture of naive $CD4^+$ T cells with DCs that were left unstimulated (iDC) or primed for 48 h with curdlan, *C. albicans*, LPS and/or *F. monophora*. In (a,b), DC-induced IL-12 secretion was abrogated by IRF1 silencing, while in (c,d), T cell stimulation by IL-12 was blocked by neutralizing IL-12 antibodies during DC-T cell coculture. In (b,d,f), the % IL-4- and IFN-γ-producing T cells are shown, corresponding to the upper left and lower right quadrants of (a,c,e), respectively. Data are presented as mean ± SD of duplicates (b,d,f,g). Data are representative of at least two (a,b,g), three (c,d) or eight (e,f) independent experiments.

chromoblastomycosis to restrict generation of protective TH1 immunity. In fact, the CD4+ T cell effector response induced by these virulent fungi was dominated by TH2 cells. TH2-biased immunity causes severe suppression of phagocytic effector cell function, and hence has adverse effects on fungal infections[4,47]. Therefore, TH2 predomination and impaired TH1 responses might represent a central immunological 'defect' in chromoblastomycosis that contributes to the establishment of chronic subcutaneous infections.

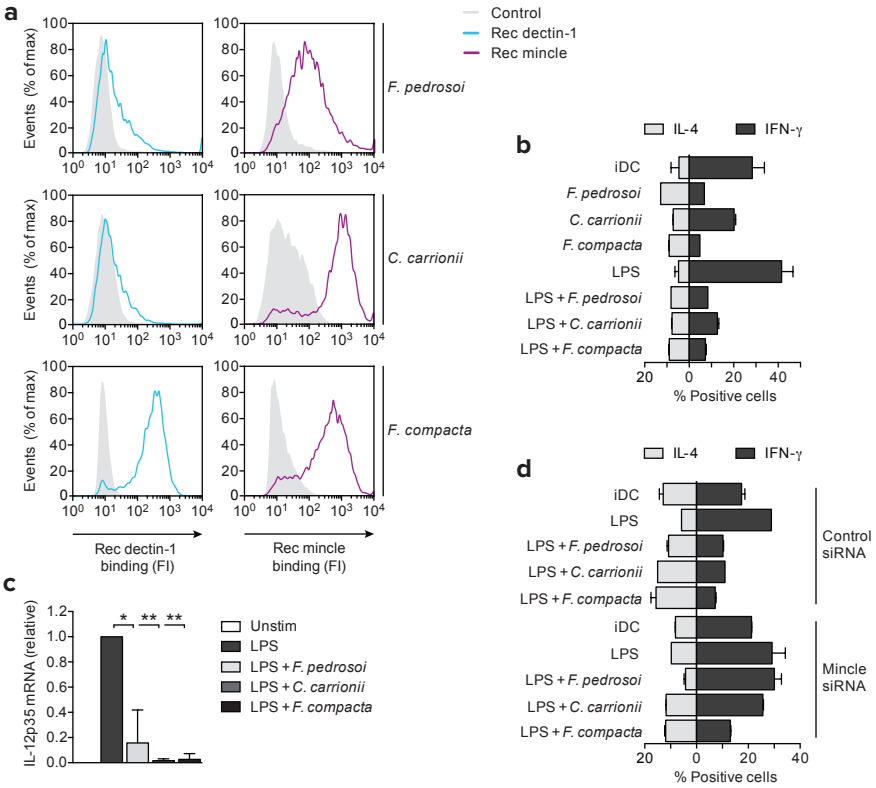

Figure 7. Pathogenic chromoblastomycosis-related fungi redirect TH polarization via mincle. (a) Binding of recombinant dectin-1 (*blue*) or mincle (*pink*) protein to heat-killed *F. pedrosoi*, *C. carrionii* or *F. compacta* conidia, determined by flow cytometry (FI, fluorescence intensity). (b,d) T helper cell polarization was determined by flow cytometry by staining for intracellular IL-4 (TH2) or IFN-γ (TH1) expression after coculture of naive CD4+ T cells with DCs that were left unstimulated (iDC) or primed for 48 h with LPS and/or *F. pedrosoi*, *C. carrionii* or *F. compacta*, after mincle silencing. Data are presented as mean ± SD of duplicates. (c) IL-12p35 mRNA expression in DCs 6 h after stimulation with LPS and/or *F. pedrosoi*, *C. carrionii* or *F. compacta*, measured by real-time PCR, normalized to GAPDH and set at 1 in LPS-stimulated cells. Data are presented as mean ± SD. **P* < 0.05; ***P* < 0.01. Data are representative of at least two (a,b,d) or three (c) independent experiments.

Overall, our study has identified an essential role for mincle in shaping overall adaptive immunity to virulent fungi associated with chromoblastomycosis. Therapeutic targeting of mincle may therefore prove beneficial not only in treatment of chromoblastomycosis, but also diseases marked by uncontrolled IL-12-driven inflammation.

EXPERIMENTAL PROCEDURES

Cells, stimuli, RNA interference and maturation. $CD14^+$ monocytes from healthy volunteer blood donors were isolated cultured and differentiated into immature DCs as described[17] and used at day 6 or 7 for experiments. Donors were routinely screened for dectin-1 single nucleotide polymorphism rs16910526 using TaqMan genotyping Assays (Assay ID C_33748481_10; Applied Biosystems); only dectin-1 wild-type DCs were used for experiments, unless otherwise indicated. This study was done in accordance with ethical guidelines of the Academic Medical Center. Cell surface expression of CLRs and maturation markers were determined as described in Supplemental Experimental Procedures. Cells were stimulated with TLR and CLR ligands and fungal pathogens in the presence or absence of signaling inhibitors as described in Supplemental Experimental Procedures. DCs were transfected with 25 nM siRNA using transfection reagens DF4 (Dharmacon) as described[17]. Details on the SMARTpool siRNAs used can be found in Supplemental Experimental Procedures. Silencing of expression was verified by real-time PCR and flow cytometry (Figure S3 and[27]).

CLR-fungi binding. Recombinant human His-tagged dectin-1 (1859-DC-50; R&D Systems) and DDK-tagged mincle (TP300244; Origene) were incubated with heat-killed fungal conidia, and subsequently labeled with anti-His-tag (sc-8036; Santa Cruz) or anti-DDK-tag (TA50011-100; Origene), respectively, followed by incubation with Alexa Fluor 488-conjugated anti-mouse (A11029; Invitrogen). CLR-fungi inding was analyzed on a FACS Calibur (BD).

Cytokine production. Cell culture supernatants were harvested after 24 h of stimulation and concentrations of IL-6, IL-23, IL-1β, IL-12p40 (Invitrogen), and IL-12p70 (eBioscience) were determined by ELISA.

Quantitative real-time PCR. mRNA isolation from DCs stimulated for 6 h, cDNA synthesis and PCR amplification with the SYBR Green method in an ABI 7500 Fast PCR detection system (Applied Biosystems) were performed as described[17]. Specific primers were designed with Primer Express 2.0 (Applied Biosystems; Table S1). The C_t value is defined as the number of PCR cycles where the fluorescence signal exceeds the detection threshold value. For each sample, the normalized amount of target mRNA N_t was calculated from the obtained C_t values for both target and GAPDH mRNA with $N_t = 2^{Ct\,(GAPDH)-Ct\,(target)}$. The relative mRNA expression was obtained by setting N_t in LPS- or curdlan-stimulated samples at 1 within one experiment and for each donor.

NF-κB DNA binding. Nuclear and cytoplasmic extracts of DCs were prepared after 2 h of stimulation using NucBuster protein extraction kit (Novagen). NF-κB DNA binding was determined using TransAM NF-κB family kit (Active Motif).

Chromatin immunoprecipitation (ChIP) assay. ChIP assays were performed using the ChIP-IT Express Enzymatic Shearing and ChIP-IT Express HT kits (both from Active Motif). Briefly, cells were fixed with 1% (vol/vol) *para*-formaldehyde after 2 h of stimulation, nuclei were isolated and chromatin DNA fragmented by enzymatic shearing (10 min, 37°C). Protein-DNA complexes were immunoprecipitated and DNA was purified after reversal of crosslinks. Details are described in Supplemental Experimental Procedures. Real-time PCR reactions were performed with primer sets spanning TATA box, NF-κB and ISRE binding sites (Table S1). Primers spanning genomic DNA at cytogenetic location 12 p13.3 (Active Motif) were used as a negative control. To normalize for DNA input, a sample for each condition was taken along which had not undergone immunoprecipitation ('input DNA'); results are expressed as % input DNA.

Chromatin accessibility real-time PCR (ChART) assay. ChART assays were performed to measure *IL12A* nucleosome remodeling as described previously[48]. Details are described in Supplemental Experimental Procedures. Briefly, nuclei were isolated after 3 h of stimulation, digested with *Bst*XI or *Eco*RI, and DNA was purified. Real-time PCR reactions were performed with primer sets spanning (A) *Bst*XI site located at nt -298 that becomes available after nuc-2 remodeling, (B) *Bst*XI site located at nt 456 that is not subject to chromatin alterations as an internal control[31], (c) GAPDH to normalize for DNA input (Table S1). Results are expressed as % remodeling observed in the *Eco*RI-digested sample for each cell treatment using the formula $(Nt_{EcoRI} - Nt_{BstXI})/Nt_{EcoRI} \times 100\%$, with $Nt = 2^{Ct(c)-Ct(A)}$.

Cellular localization and association of Mdm2 and IRF1. Nuclear and cytoplasmic extracts of DCs were prepared after 2 h of stimulation using NucBuster protein extraction kit (Novagen). For detection of association between Mdm2 and IRF1, extracts were prepared from DCs stimulated in the presence of proteasome inhibitor MG-132. Mdm2-IRF1 complexes were immunoprecipitated from 20 µg of nuclear extract with anti-IRF1 (sc-497; Santa Cruz) coated on protein A/G-PLUS agarose beads (Santa Cruz). Proteins were resolved by SDS-PAGE, and Mdm2 and IRF1 were detected by immunoblotting. Details are described in Supplemental Experimental Procedures. IRF1 was also detected in extracts by ELISA (USCN Life Science). IRF1 localization was further determined by immunofluorescense staining: DCs were stimulated, fixed with 4% *para*-formaldehyde, then permeabilized with 0.2% (vol/vol) Triton X-100 in PBS, and stained with anti-IRF1. Incubation of Alexa Fluor 594-conjugated anti-rabbit (A11072; Molecular Probes) was followed by staining of nuclei with DAPI (Molecular Probes). IRF1 localization was visualized with a Leica DMR A microscope.

PKB and Mdm2 phosphorylation. Phosphorylation of PKB and Mdm2 after 20 min of stimulation was detected by flow cytometry and analyzed on a FACS Calibur (BD). Details are described in Supplemental Experimental Procedures. Phosphorylated Mdm2 was also detected by immunoblotting as described above.

PKB activity assay. Whole cell extracts were prepared after 30 min of stimulation in kinase activity lysis buffer as described[49]. PKB kinase activity was measured using PKB kinase activity kit (Enzo Life Science); details are described in Supplemental Experimental Procedures.

T cell differentiation assay. DCs were silenced for indicated proteins, activated for 48 h with LPS and/or heat-killed fungal strains and subsequently cocultured with naive $CD4^+$ T cells as described[50]. Neutralizing IL-12 antibodies (MAB219; R&D) were added at this point as indicated. Details are described in Supplemental Experimental Procedures. After restimulation with 100 ng/ml PMA (Sigma) and 1 μg/ml ionomycin (Sigma), intracellular cytokine expression was analyzed by flow cytometry by staining with APC-conjugated rat anti-IL-4 (MP4-25D2) and FITC-conjugated mouse anti-IFN-γ (25723.11; both BD).

Statistical analysis. Statistical analyses were performed on the data using the Student's *t* test for paired observations. Statistical significance was set at $P < 0.05$.

REFERENCES

1. Queiroz-Telles, F. *et al.* Chromoblastomycosis: an overview of clinical manifestations, diagnosis and treatment. Med. Mycol. 47, 3-15 (2009).

2. Sousa Mda, G. *et al.* Restoration of pattern recognition receptor costimulation to treat chromoblastomycosis, a chronic fungal infection of the skin. Cell host & microbe 9, 436-443 (2011).

3. Roy, R.M. & Klein, B.S. Dendritic cells in antifungal immunity and vaccine design. Cell host & microbe 11, 436-446 (2012).

4. Wuthrich, M., Deepe, G.S., Jr. & Klein, B. Adaptive immunity to fungi. Annu. Rev. Immunol. 30, 115-148 (2012).

5. Romani, L. Immunity to fungal infections. Nat. Rev. Immunol. 11, 275-288 (2011).

6. Brown, G.D. Innate antifungal immunity: the key role of phagocytes. Annu. Rev. Immunol. 29, 1-21 (2011).

7. Korn, T., Bettelli, E., Oukka, M. & Kuchroo, V.K. IL-17 and Th17 Cells. Annu. Rev. Immunol. 27, 485-517 (2009).

8. De Luca, A. *et al.* IL-22 defines a novel immune pathway of

antifungal resistance. Mucosal Immunol. 3, 361-373 (2010).

9. Schroder, K., Hertzog, P.J., Ravasi, T. & Hume, D.A. Interferon-gamma: an overview of signals, mechanisms and functions. J. Leukoc. Biol. 75, 163-189 (2004).

10. Zielinski, C.E. *et al.* Pathogen-induced human Th17 cells produce IFN-gamma or IL-10 and are regulated by IL-1beta. Nature 484, 514-518 (2012).

11. Moser, M. & Murphy, K.M. Dendritic cell regulation of Th1-Th2 development. Nat. Immunol. 1, 199-205 (2000).

12. Geijtenbeek, T.B. & Gringhuis, S.I. Signalling through C-type lectin receptors: shaping immune responses. Nat. Rev. Immunol. 9, 465-479 (2009).

13. Hardison, S.E. & Brown, G.D. C-type lectin receptors orchestrate antifungal immunity. Nat. Immunol. 13, 817-822 (2012).

14. Gringhuis, S.I. *et al.* Dectin-1 directs T helper cell differentiation by controlling noncanonical NF-kappaB activation through Raf-1 and Syk. Nat. Immunol. 10, 203-213 (2009).

15. Gringhuis, S.I. *et al.* Selective C-Rel activation via Malt1 controls anti-fungal T(H)-17 immunity by dectin-1 and dectin-2. PLoS Pathog. 7, e1001259 (2011).

16. Gross, O. *et al.* Card9 controls a non-TLR signalling pathway for innate anti-fungal immunity. Nature 442, 651-656 (2006).

17. Yamasaki, S. *et al.* C-type lectin Mincle is an activating receptor for pathogenic fungus, Malassezia. Proc. Natl. Acad. Sci. U. S. A. 106, 1897-1902 (2009).

18. Wells, C.A. *et al.* The macrophage-inducible C-type lectin, mincle, is an essential component of the innate immune response to Candida albicans. J. Immunol. 180, 7404-7413 (2008).

19. Yamasaki, S. *et al.* Mincle is an ITAM-coupled activating receptor that senses damaged cells. Nat. Immunol. 9, 1179-1188 (2008).

20. Strasser, D. *et al.* Syk kinase-coupled C-type lectin receptors engage protein kinase C-sigma to elicit Card9 adaptor-mediated innate immunity. Immunity 36, 32-42 (2012).

21. Ishikawa, E. *et al.* Direct recognition of the mycobacterial glycolipid, trehalose dimycolate, by C-type lectin Mincle. J. Exp. Med. 206, 2879-2888 (2009).

22. Schoenen, H. *et al.* Cutting edge: Mincle is essential for recognition and adjuvanticity of the mycobacterial cord factor and its synthetic analog trehalose-dibehenate. J. Immunol. 184, 2756-2760 (2010).

23. Hunter, C.A. New IL-12-family members: IL-23 and IL-27, cytokines with divergent functions. Nat. Rev. Immunol. 5, 521-531 (2005).

24. Ferwerda, B. *et al.* Human dectin-1 deficiency and mucocutaneous fungal infections. N. Engl. J. Med. 361, 1760-1767 (2009).

25. Sarbassov, D.D., Guertin, D.A., Ali, S.M. & Sabatini, D.M. Phosphorylation and regulation of Akt/PKB by the rictor-mTOR complex. Science 307, 1098-1101 (2005).

26. Goriely, S. *et al.* Human IL-12(p35) gene activation involves selective remodeling of a single nucleosome within a region of the promoter containing critical Sp1-binding

sites. Blood 101, 4894-4902 (2003).

27. Goriely, S. *et al.* A defect in nucleosome remodeling prevents IL-12(p35) gene transcription in neonatal dendritic cells. J. Exp. Med. 199, 1011-1016 (2004).

28. Liu, J., Cao, S., Herman, L.M. & Ma, X. Differential regulation of interleukin (IL)-12 p35 and p40 gene expression and interferon (IFN)-gamma-primed IL-12 production by IFN regulatory factor 1. J. Exp. Med. 198, 1265-1276 (2003).

29. Nakagawa, K. & Yokosawa, H. Degradation of transcription factor IRF-1 by the ubiquitin-proteasome pathway. The C-terminal region governs the protein stability. Eur. J. Biochem. 267, 1680-1686 (2000).

30. Landre, V., Pion, E., Narayan, V., Xirodimas, D.P. & Ball, K.L. DNA-binding regulates site-specific ubiquitination of IRF-1. Biochem. J. 449, 707-717 (2013).

31. Mayo, L.D. & Donner, D.B. A phosphatidylinositol 3-kinase/Akt pathway promotes translocation of Mdm2 from the cytoplasm to the nucleus. Proc. Natl. Acad. Sci. U. S. A. 98, 11598-11603 (2001).

32. Zhou, B.P. *et al.* HER-2/neu induces p53 ubiquitination via Akt-mediated MDM2 phosphorylation. Nat. Cell Biol. 3, 973-982 (2001).

33. Haupt, Y., Maya, R., Kazaz, A. & Oren, M. Mdm2 promotes the rapid degradation of p53. Nature 387, 296-299 (1997).

34. Yang, J.Y. *et al.* ERK promotes tumorigenesis by inhibiting FOXO3a via MDM2-mediated degradation. Nat. Cell Biol. 10, 138-148 (2008).

35. Ishikawa, T. *et al.* Identification of Distinct Ligands for the C-type Lectin Receptors Mincle and Dectin-2 in the Pathogenic Fungus Malassezia. Cell host & microbe 13, 477-488 (2013).

36. LeibundGut-Landmann, S. *et al.* Syk- and CARD9-dependent coupling of innate immunity to the induction of T helper cells that produce interleukin 17. Nat. Immunol. 8, 630-638 (2007).

37. Holten-Andersen, L., Doherty, T.M., Korsholm, K.S. & Andersen, P. Combination of the cationic surfactant dimethyl dioctadecyl ammonium bromide and synthetic mycobacterial cord factor as an efficient adjuvant for tuberculosis subunit vaccines. Infect. Immun. 72, 1608-1617 (2004).

38. Agger, E.M. *et al.* Cationic liposomes formulated with synthetic mycobacterial cordfactor (cAF01): a versatile adjuvant for vaccines with different immunological requirements. PLoS One 3, e3116 (2008).

39. Lang, R., Schoenen, H. & Desel, C. Targeting Syk-Card9-activating C-type lectin receptors by vaccine adjuvants: findings, implications and open questions. Immunobiology 216, 1184-1191 (2011).

40. Gautier, G. *et al.* A type I interferon autocrine-paracrine loop is involved in Toll-like receptor-induced interleukin-12p70 secretion by dendritic cells. J. Exp. Med. 201, 1435-1446 (2005).

41. Tamura, T., Yanai, H., Savitsky, D. & Taniguchi, T. The IRF family transcription factors in immunity and oncogenesis. Annu. Rev. Immunol. 26, 535-584 (2008).

42. Negishi, H. *et al.* Evidence for licensing of IFN-gamma-induced IFN regulatory factor 1 transcription factor by MyD88 in Toll-like receptor-dependent gene induction program. Proc.

Natl. Acad. Sci. U. S. A. 103, 15136-15141 (2006).

43. Cheng, J., Phong, B., Wilson, D.C., Hirsch, R. & Kane, L.P. Akt fine-tunes NF-kappaB-dependent gene expression during T cell activation. J. Biol. Chem. 286, 36076-36085 (2011).

44. Lionakis, M.S. & Kontoyiannis, D.P. Glucocorticoids and invasive fungal infections. Lancet 362, 1828-1838 (2003).

45. Boguniewicz, M. & Leung, D.Y. Atopic dermatitis: a disease of altered skin barrier and immune dysregulation. Immunol. Rev. 242, 233-246 (2011).

46. Wick, G. *et al.* The immunology of fibrosis. Annu. Rev. Immunol. 31, 107-135 (2013).

47. d'Avila, S.C., Pagliari, C. & Duarte, M.I. The cell-mediated immune reaction in the cutaneous lesion of chromoblastomycosis and their correlation with different clinical forms of the disease. Mycopathologia 156, 51-60 (2003).

48. Gringhuis, S.I. *et al.* C-type lectin DC-SIGN modulates Toll-like receptor signaling via Raf-1 kinase-dependent acetylation of transcription factor NF-kappaB. Immunity 26, 605-616 (2007).

49. Hovius, J.W. *et al.* Salp15 binding to DC-SIGN inhibits cytokine expression by impairing both nucleosome remodeling and mRNA stabilization. PLoS Pathog. 4, e31 (2008).

50. de Jong, E.C. *et al.* Microbial compounds selectively induce Th1 cell-promoting or Th2 cell-promoting dendritic cells in vitro with diverse th cell-polarizing signals. J. Immunol. 168, 1704-1709 (2002).

SUPPLEMENTAL EXPERIMENTAL PROCEDURES

Cells, stimuli, inhibitors, fungal strains and RNA interference. Cell surface expression of dectin-1, mincle and MCL was determined by flow cytometry analysis with anti-dectin-1 (MAB1859; R&D Systems), anti-mincle (clone 2D12; Abnova) and anti-MCL (clone 41312; R&D Systems), respectively. Maturation of DCs was determined by cell surface expression analysis by flow cytometry of CD80 (557227; BD), CD86 (PN1M2218; Beckmann Coulter), CD83 (555658; BD) and HLA-DR (FAB18381P; R&D). Cells were stimulated with 10 mg/ml curdlan, 10 ng/ml *Salmonella typhosa* LPS (both from Sigma) or 0.2 mg/ml TDB (Avanti Polar Lipids) as previously described1. Cells were preincubated with blocking antibodies or inhibitor for 2 h with 20 μg/ml anti-dectin-1 (MAB1859; R&D Systems), 0.5 mM wortmannin (PI3K inhibitor), 5 mM triciribine (PKB inhibitor),100 nM MG-132 (proteasome inhibitor; all Calbiochem). DCs were transfected with 25 nM siRNA using transfection reagens DF4 (Dharmacon) as described2.SMARTpool siRNAs used were: Mincle (M-021374-02), MCL (M-021373-00), Syk (M-003176-03), CARD9 (M-004400-01), Bcl-10 (M-004381-02), MALT1 (M-005936-02), IRF1 (M-011704-01), PKB (M-003000-03), Mdm2 (M-003279-04) and non-targeting siRNA (D-001206-13) as a control (Dharmacon). *Candida* albicans strain CBS2712 was grown in Sabouraud dextrose broth and incubated for 3 d at 25°C, while shaking. Conidia were dislodged from slants by gentle tapping and then were resuspended in 0.1% (vol/vol) Tween-80 in PBS. *Fonsecaea* and Cladophialophora strains (*F. monophora* CBS269.30, *F. pedrosoi* CBS271.37, *F. compacta* CBS285.47 and *C. carrionii* CBS109.97) were grown for 7 d at 37°C on Oatmeal agar culture plates. 0.1% Tween-80 in PBS was used to remove and resuspend the grown conidia. Hyphal contamination was removed by straining of the cell solutions through a glass filter. Swollen germinating conidia were obtained by incubation for 6 h at 37°C, with shaking, in 0.1% (vol/vol) Tween-80 in PBS. Fungi were inactivated by being heated for 1 h at 56°C. Live fungi were used when indicated. DCs were stimulated with fungi at multiplicity of infection (MOI) 5.

Chromatin immunoprecipitation (ChIP) assay. Protein-DNA complexes were immunoprecipitated using anti-p65 (3034; Cell Signaling), anti-RNAPII (4H8; Active Motif), anti-IRF1 (c-20) or negative control IgG (sc-2027; Santa Cruz), and protein G-coated magnetic beads.

Chromatin accessibility real-time PCR (ChART) assay. Nuclei were prepared with lysis buffer (10 mM Tris-HCl, pH 7.5; 15 mM NaCl; 3 mM MgCl2; 0.5 mM spermidine; 0.15 mM spermine; 1 mM PMSF; 0.5 % (vol/vol) Nonidet P-40). Digestion reactions were performed with 50 U BstIXI or 50 U EcoRI for 1 h at 37°C. After proteinase K and RNase A treatment, DNA was purified using the QIAamp DNA blood kit (QiaGen).

Cellular localization and association of Mdm2 and IRF1 by immunoblotting. Nuclear and cytoplasmic extracts and immunoprecipitates were resolved by SDS-PAGE, and detected by immunoblotting with anti-Mdm2 (ab38618; Abcam), anti-phospho-Mdm2 (S166) (ab58532; Abcam) or anti-IRF1 (ab26109; Abcam). Membranes were also probed with anti-RNAPII (clone CTD4H8; Millipore) or anti-b-actin (sc-81178; Santa Cruz) to ensure equal protein loading among cytoplasmic and nuclear extracts, respectively. Primary antibody incubation was followed by incubation with HRP-conjugated secondary antibody (rabbit: 21230; Pierce, or mouse: P0161, DAKO) and ECL detection (Pierce).

PKB and Mdm2 phosphorylation by FACS. Cells were first fixed in 3% para-formaldehyde for 10 min and permeabilized in 90% methanol at 4°C for 30 min. Primary antibody incubation with anti-phospho-PKB (T308) (2965; Cell Signaling), anti-phospho-PKB (S473) (4060; Cell Signaling) and anti-phospho-Mdm2 (S166) (ab58532; Abcam) was followed by incubation with PE-conjugated anti-rabbit (711-116-152; Jackson Immunoresearch). Phosphorylation was analyzed on a FACS Calibur (BD).

PKB activity assay. DCs were stimulated for 30 min and whole cell extracts were prepared in kinase activity lysis buffer as described2. PKB kinase activity was measured using PKB kinase activity kit (Enzo Life Science). Briefly, 60 mg cell extract was incubated in wells precoated with a PKB substrate in the presence of ATP for 90 min at 30°C. Phosphorylation of the peptide substrate was assayed using a phospso-specific substrate antibody, followed by incubation with HRP-conjugated anti-rabbit IgG; absorbance detection at 450 nm is a measure for PKB kinase activity.

T cell differentiation assay. Naive $CD4^+$ T cells were isolated with MACS beads isolation as described previously (de Jong et al., 2002). DCs were silenced for indicated proteins, activated for 48 h with LPS and/or heat-killed fungal strains and subsequently cocultured with naive $CD4^+$ T cells (20,000 T cells/5000 DCs) in the presence of Staphylococcus aureus enterotoxin B (10 pg/ml; Sigma). Neutralizing IL-12 antibodies (MAB219; R&D) were added at this point as indicated to block T cell stimulation by IL-12. DCs primed with LPS plus IFN-g (1000 U/ml; U-CyTech) or prostaglandin E2 (1 mM; Sigma) were used as positive controls for T_H1 or T_H2 differentiation, respectively. After 5 days of coculture, cells were further cultured in the presence of IL-2 (10 U/ml; Chiron). Resting cells were restimulated after 12-17 days with PMA (100 ng/ml) and ionomycin (1 mg/ml) for 6 h, the last 4 h in the presence of brefeldin A (10 mg/ml; all Sigma). Intracellular cytokine expression was analyzed by staining with FITC-conjugated mouse anti-IFN-γ (25723.11) and APC-conjugated rat anti-IL-4 (MP4-25D2; both BD).

SUPPLEMENTAL FIGURES

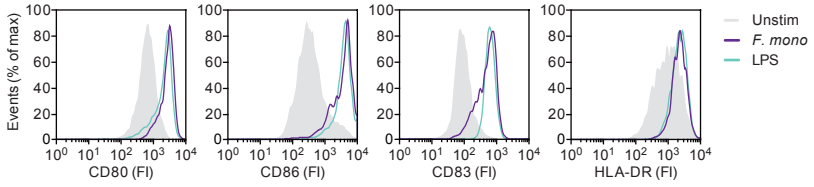

Figure S1, related to Figure 1. Maturation of human primary DCs. Expression of maturation markers CD80, CD86, CD83 and HLA-DR on DCs left unstimulated (*grey*) or 24 h after stimulation with *F. monophora* (*purple*) or LPS (*green*), determined by flow cytometry (FI, fluorescence intensity). Data are representative of at least two independent experiments.

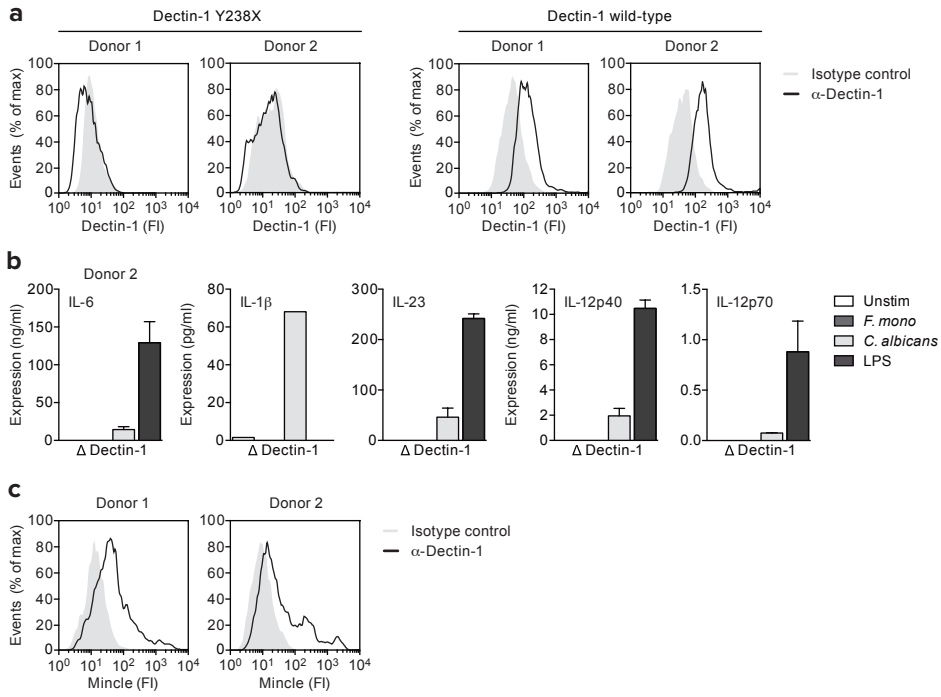

Figure S2, related to Figure 1. Dectin-1 and mincle expression on human primary DCs. (a) Dectin-1 expression on primary immature DCs from two individuals carrying a homozygous Y238X mutation in dectin-1 (*left*), hence lacking functional dectin-1, and two donors with wild-type dectin-1 (*right*), determined by flow cytometry (FI, fluorescence intensity). (b) Cytokine secretion in supernatants of DCs from donor (2) lacking functional dectin-1, due to a homozygous dectin-1 Y238X mutation, 24 h after stimulation with curdlan, LPS and/or *F. monophora* or *C. albicans* measured by ELISA. Together with data in Figure 1g, these data are representative of two independent experiments. (c) Mincle expression on primary immature DCs, determined by flow cytometry (FI, fluorescence intensity). Data are representative of at least three independent experiments.

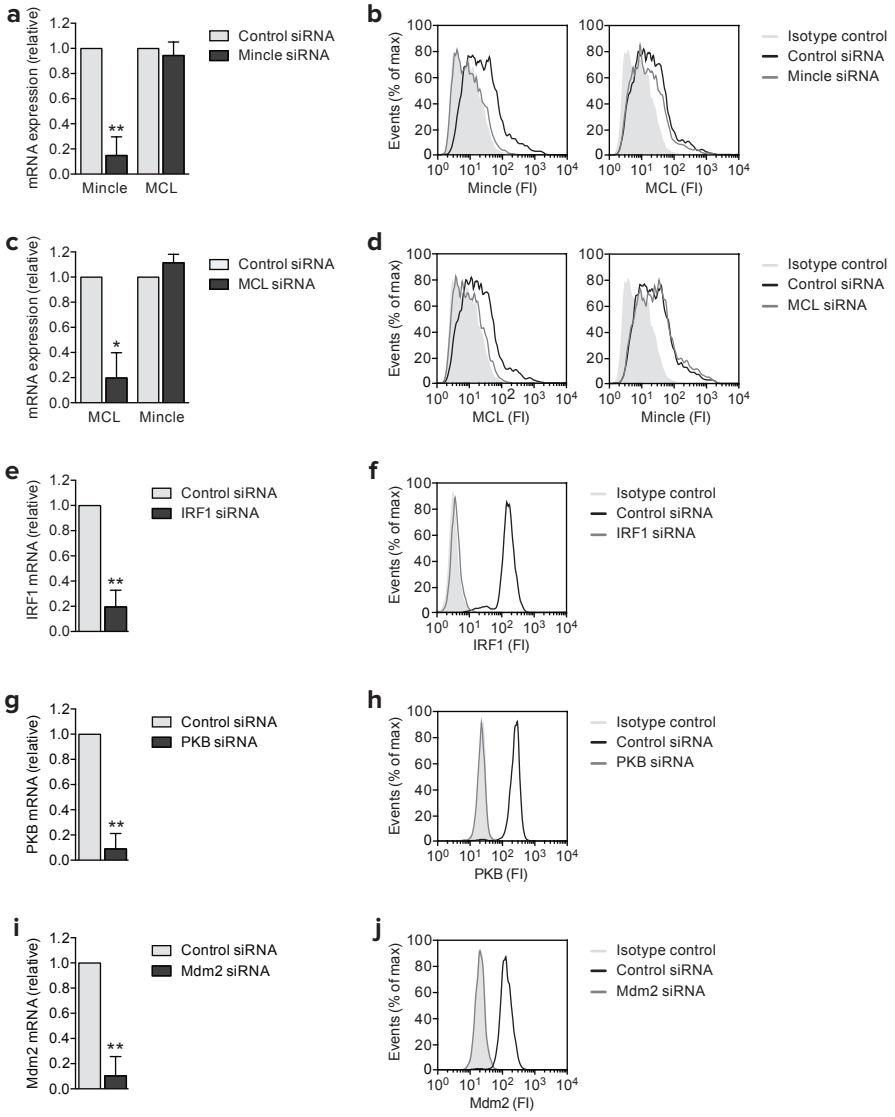

Figure S3, related to Figures 1-7. Silencing of mincle, MCL, IRF1, PKB and Mdm2 in human primary DCs by RNA interference. (a-j) Silencing of indicated proteins using specific SMARTpools and non-targeting siRNA as a control. Silencing was confirmed by real-time PCR (a,c,e,g,i) or flow cytometry (b,d,f,h,j; FI, fluorescence intensity). In (a,c,e,g,i), mRNA expression was normalized to GAPDH and set at 1 in control siRNA-treated cells. Data are presented as mean ± SD. $*P < 0.05$, $**P < 0.01$. Antibodies used for staining are anti-mincle (clone 2D12; Abnova) (b,d), anti-MCL (clone 41312; R&D Systems) (b,d), anti-IRF1 (sc-497; Santa Cruz) (f), anti-PKB (ab32505; Abcam) (h) and anti-Mdm2 (ab38618; Abcam) (j). Data are representative of at least three independent experiments.

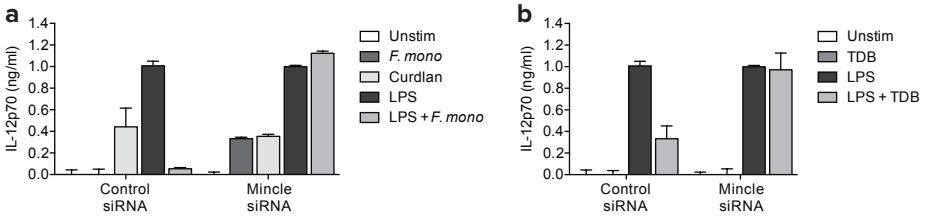

Figure S4, related to Figure 1. Mincle silencing reverses *F. monophora*- or TDB-mediated suppression of IL-12p70 expression by human primary DCs. (a,b) Cytokine secretion in supernatants of DCs 24 h after stimulation with curdlan, LPS and/or *F. monophora* or TDB, after mincle silencing by RNA interference (siRNA), measured by ELISA. Data are presented as mean ± SD of duplicates samples and representative of three independent experiments.

Figure S5, related to Figure 2 and 5. TLR4 does not induce PKB or Mdm2 phosphorylation, while mincle-induced Mdm2 phosphorylation is dependent on Syk-CARD9-Bcl-10-MALT1 signaling. (a-d) Flow cytometry analysis (FI, fluorescence intensity) of PKB phosphorylation at Thr308 or Ser473 (a,b), or Mdm2 phosphorylation at Ser166 (c,d) in DCs left unstimulated (*filled grey*), or stimulated with LPS (*green*), curdlan (*blue*), TDB (*orange*), LPS plus TDB (*pink*), or *F. monophora* (*purple*), in the absence or presence of Syk inhibitor piceatannol, PI(3)K-inhibitor wortmannin or PKB inhibitor triciribine, or after mincle, Syk, CARD9, Bcl-10 or MALT1 silencing. Data are representative of at least two (b) or three (a,c,d) independent experiments.

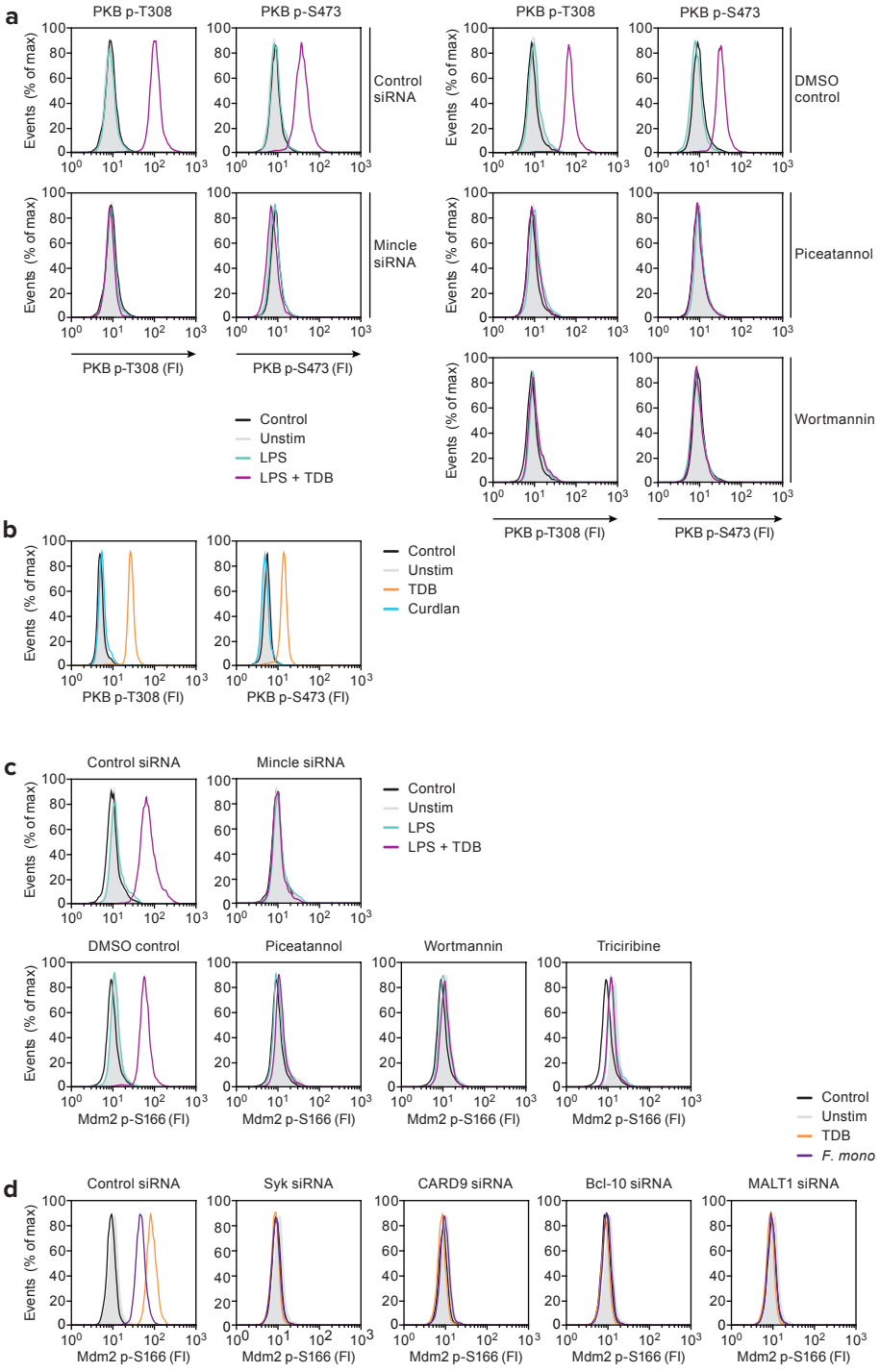
a
PKB p-T308
PKB p-S473
Events (% of max)
Control siRNA
Mincle siRNA
DMSO control
Piceatannol
Wortmannin
PKB p-T308 (FI)
PKB p-S473 (FI)
Control
Unstim
LPS
LPS + TDB
b
TDB
Curdlan
c
Control siRNA
Mincle siRNA
DMSO control
Piceatannol
Wortmannin
Triciribine
Mdm2 p-S166 (FI)
F. mono
d
Syk siRNA
CARD9 siRNA
Bcl-10 siRNA
MALT1 siRNA

SUPPLEMENTAL TABLE

Expression primer sequences		
Gene product	**Forward primer (5'-3')**	**Reverse primer (5'-3')**
Bcl-10	ATGGAGCCACGAACAACCTCT	TCGTGCTGGATTCTCCTTCTG
CARD9	CATGTCGGACTACGAGAACGAT	CAGGTAAGGTGTGATGCGTGA
GAPDH	CCATGTTCGTCATGGGTGTG	GGTGCTAAGCAGTTGGTGGTG
IL-1β	TTTGAGTCTGCCCAGTTCCC	TCAGTTATATCCTGGCCGCC
IL-6	TGCAATAACCACCCCTGACC	TGCGCAGAATGAGATGAGTTG
IL-12p35	CTCCAGAAGGCCAGACAAAC	AATGGTAAACAGGCCTCCACT
IL-12p40	CCAGAGCAGTGAGGTCTTAGGC	TGTGAAGCAGCAGGAGCG
IL-23p19	GCTTGCAAAGGATCCACCA	TCCGATCCTAGCAGCTTCTCA
IRF1	TTATACAGTGCCTTGCTCGGC	AGGCGCTCACACTTCCCTC
MALT1	GACCCATTCCATGGTGTTTACC	AATAAATGCATCTGGAGTCCGG
MCL	TGGCATAAGAATGAACCCGAC	TCCAGGCCCATTTATCTTGG
Mdm2	ATCAGAACCCCCACTCACCC	TGCCTCGCTCTCTTCCTACAAC
Mincle	CTCACAGGAGGAGCAGGAATTC	TGACCCTCGACAACCTGGTC
PKB	AGAAGGACCCCAAGCAGAGG	CACGATACCGGCAAAGAAGC
Syk	CCAGAGACAACAACGGCTCC	TGTCGATGCGATAGTGCAGC

ChIP primer sequences		
Gene target	**Forward primer (5'-3')**	**Reverse primer (5'-3')**
IL12A TATA box	CGCACGTGTCACCGAGAA	GGGACTCTGGTCTCTTGCTTTC
IL12A NF-κB	GAGTACTCAGCCCGCCAGG	CCTCTTTGCAGGAGACGGC
IL12A ISRE (ref [5])	GCGAACATTTCGCTTTCATT	ACTTTCCCGGGACTCTGGT

ChART primer sequences			
Set	**Target**	**Forward primer (5'-3')**	**Reverse primer (5'-3')**
A	*IL12A* prom	GCGGGGTAGCTTAGACACG	CCCAAAATGAAAGCGAAATG
B	*IL12A* BstXI contr	TCTAAAGTCAGGCTTGGCCG	GGTTTCACCATGTTGGTCAGG
C	*GAPDH* prom	TACTAGCGGTTTTACGGGCG	TCGAACAGGAGGAGCAGAGAGCGA

SUPPLEMENTAL REFERENCES

1. Ishikawa, E., Ishikawa, T., Morita, Y.S., Toyonaga, K. *et al.* Direct recognition of the mycobacterial glycolipid, trehalose dimycolate, by C-type lectin Mincle. J. Exp. Med. 206, 2879-2888 (2009).

2. Gringhuis, S.I., den Dunnen, J., Litjens, M., van der Vlist, M. *et al.* Dectin-1 directs T helper cell differentiation by controlling noncanonical NF-kappaB activation through Raf-1 and Syk. Nat. Immunol. 10, 203-213 (2009).

3. Gringhuis, S.I., den Dunnen, J., Litjens, M., van Het Hof, B. *et al.* C-type lectin DC-SIGN modulates Toll-like receptor signaling via Raf-1 kinase-dependent acetylation of transcription factor NF-kappaB. Immunity 26, 605-616 (2007).

4. de Jong, E.C., Vieira, P.L., Kalinski, P., Schuitemaker, J.H. *et al.* Microbial compounds selectively induce Th1 cell-promoting or Th2 cell-promoting dendritic cells in vitro with diverse th cell-polarizing signals. J. Immunol. 168, 1704-1709 (2002).

5. Goodall, J.C., Wu, C., Zhang, Y., McNeill, L. *et al.* Endoplasmic reticulum stress-induced transcription factor, CHOP, is crucial for dendritic cell IL-23 expression. Proc. Natl. Acad. Sci. U. S. A. 107, 17698-17703 (2010).

This work was supported by the Netherlands Organisation for Scientific Research (NGI 40-41009-98-8057 to S.I.G.; VICI 918.10.619 to T.B.H.G.).